Journal of Power Sources 183 (2008) 479–484

Contents lists available at ScienceDirect

Journal of Power Sources

journal homepage: www.elsevier.com/locate/jpowsour

Stable, easily sintered $BaCe_{0.5}Zr_{0.3}Y_{0.16}Zn_{0.04}O_{3-\delta}$ electrolyte-based protonic ceramic membrane fuel cells with $Ba_{0.5}Sr_{0.5}Zn_{0.2}Fe_{0.8}O_{3-\delta}$ perovskite cathode

Bin Lin [a], Mingjun Hu [a], Jianjun Ma [a], Yinzhu Jiang [a,b], Shanwen Tao [b], Guangyao Meng [a,*]

[a] Department of Materials Science and Engineering, University of Science and Technology of China (USTC), 96 Jinzhai Road, Hefei, Anhui 230026, PR China
[b] Department of Chemistry, School of Engineering and Physical Sciences, Heriot-Watt University, Edinburgh EH14 4AS, UK

ARTICLE INFO

Article history:
Received 14 April 2008
Received in revised form 10 May 2008
Accepted 20 May 2008
Available online 3 June 2008

Keywords:
Solid oxide fuel cells
$BaCe_{0.5}Zr_{0.3}Y_{0.16}Zn_{0.04}O_{3-\delta}$
$Ba_{0.5}Sr_{0.5}Zn_{0.2}Fe_{0.8}O_{3-\delta}$
Zn dopant
Pechini method

ABSTRACT

A stable, easily sintered perovskite oxide $BaCe_{0.5}Zr_{0.3}Y_{0.16}Zn_{0.04}O_{3-\delta}$ (BCZYZn) as an electrolyte for protonic ceramic membrane fuel cells (PCMFCs) with $Ba_{0.5}Sr_{0.5}Zn_{0.2}Fe_{0.8}O_{3-\delta}$ (BSZF) perovskite cathode was investigated. The BCZYZn perovskite electrolyte synthesized by a modified Pechini method exhibited higher sinterability and reached 97.4% relative density at 1200 °C for 5 h in air, which is about 200 °C lower than that without Zn dopant. By fabricating thin membrane BCZYZn electrolyte (about 30 μm in thickness) on NiO–BCZYZn anode support, PCMFCs were assembled and tested by selecting stable BSZF perovskite cathode. An open-circuit potential of 1.00 V, a maximum power density of 236 mW cm^{-2}, and a low polarization resistance of the electrodes of 0.17 Ω cm^2 were achieved at 700 °C. This investigation indicated that proton conducting electrolyte BCZYZn with BSZF perovskite cathode is a promising material system for the next generation solid oxide fuel cells.

© 2008 Elsevier B.V. All rights reserved.

1. Introduction

The development of solid oxide fuel cells (SOFCs) has launched to a new stage characterized by thin electrolytes on porous electrode support, in which nearly all fabrication techniques developed are concerned with inorganic membranes, and hence it can also be named as ceramic membrane fuel cells (CMFCs). [1] Protonic ceramic membrane fuel cells (PCMFCs) based on proton conducting electrolytes exhibit more advantages than traditional CMFCs based on oxygen-ion conducting electrolytes, such as low activation energy [2] and high energy efficiency [3].

Now there are considerable interests in proton-conducting oxide electrolytes for PCMFCs. Many perovskite-type oxides show high proton conductivity in H_2 and/or H_2O containing atmospheres. Among the perovskite oxides, doped barium cerates exhibit mixed proton and oxide-ion conductivity [4] upon exposure to humid atmospheres. And the proton conductivity can be significantly improved by doping various rare earth ions such as Sm, Y, Yb, Eu, Gd, etc. [5–8]. Unfortunately, although much progress has been made in recent years, there are still big problems for perovskite oxide in CO_2 and steam conditions, such as poor chemical stability, which will prevent further applications in fuel cells. Compared with doped cerates, doped zirconates possess better chemical stability but lower conductivity [9]. Recent reports showed that solid solutions of $BaCeO_3$ and $BaZrO_3$ combined the high proton conductivity of barium cerate with the good chemical stability of barium zirconate [10]. However, it is difficult to get high density of zirconate and high sintering temperatures are always needed [11]. In order to solve these problems, Babilo and Haile [12] and Tao and Irvine [13] introduced Zn into Y- and Zr-doped $BaCeO_3$. Results show that Zn doping not only lowered the sintering temperature, but also increased the stability of $BaCeO_3$-based materials. This is indeed encouraging. Thus it is worthy to make cells with thin Zn-, Y-, and Zr-doped $BaCeO_3$ electrolyte and test their performance.

In order to improve materials compatibility and reduce fabrication costs, the development of proper cathode materials for PCMFCs remains to be a challenge. Many cobalt-containing perovskite-type mixed ionic–electronic conductors such as $Ba_{0.5}Sr_{0.5}Co_{0.8}Fe_{0.2}O_{3-\delta}$ [14], $Ba_{0.5}Pr_{0.5}CoO_{3-\delta}$ [15], $La_{0.5}Sr_{0.5}CoO_{3-\delta}$ [16], $La_{0.6}Ba_{0.4}CoO_{3-\delta}$ [17], $Sm_{0.5}Sr_{0.5}CoO_{3-\delta}$ [18] or $GdBaCo_2O_{5+x}$ [19] have been extensively studied as possible PCMFC cathodes. These cobalt-based cathodes in practical long-term applications often suffer some problems like poor chemical stability in CO_2, high thermal expansion coefficients (TECs), ease of evaporation and high cost of cobalt element. On the other hand, several cobalt-free perovskite oxides, such as $BaCe_{0.4}Pr_{0.4}Y_{0.2}O_{3-\delta}$ [20], $La_{0.7}Sr_{0.3}FeO_{3-\delta}$ [21], etc., have been investigated as PCMFC cathodes. Recently, $Ba_{0.5}Sr_{0.5}Zn_{0.2}Fe_{0.8}O_{3-\delta}$ (BSZF) perovskite oxide was developed by Wang et al. [22] as a novel cobalt-free oxygen-permeable membrane, which showed high permeation behavior and good chemical stability at high temperatures. Wei et al. [23,24] have also investigated the cobalt-free BSZF cathode in SOFCs based on oxide-ion

* Corresponding author. Tel.: +86 551 3606249; fax: +86 551 3607627.
E-mail address: mgym@ustc.edu.cn (G. Meng).

0378-7753/$ – see front matter © 2008 Elsevier B.V. All rights reserved.
doi:10.1016/j.jpowsour.2008.05.075

conducting electrolytes (SDC). However, to the best of our knowledge, the performance of BSZF cathodes as a part of PCMFCs has not been reported up to date. In this work, the cobalt-free BSZF synthesized by a modified Pechini method was employed as a new PCMFC cathode.

2. Experimental

The $BaCe_{0.5}Zr_{0.3}Y_{0.16}Zn_{0.04}O_{3-\delta}$ (BCZYZn) powders were synthesized by the modified Pechini method with citrate and ethylenediamine tetraacetic acid (EDTA) as parallel complexing agents. Calculated amounts of $Ba(NO_3)_2{\cdot}9H_2O$, $Ce(NO_3)_3{\cdot}6H_2O$, $Zr(NO_3)_4{\cdot}4H_2O$, Y_2O_3, ZnO (99.95%, Shanghai) were dissolved in EDTA–NH_3 aqueous solution under heating and stirring. An appropriate amount of citric acid was added in the solution. The solution was heated under stirring, converted to a viscous gel and ignited to flame, resulting in the ash. The resulting ash-like material was afterwards calcined in air at different selected temperatures (850–1100 °C) for 5 h with a fixed heating rate of 100 °C h^{-1}. The pure perovskite phase BCZYZn oxide powders calcined at 1000 °C for 5 h were held in the tube furnace at 1200 °C for 1 h with a fixed heating rate of 5 °C min^{-1} under flowing carbon dioxide for stability test. The pure BCZYZn oxide powders calcined at 1000 °C for 5 h were ball milled in an ethanol medium for 24 h and dried subsequently. Small pellets (φ15 mm × 1.5 mm) were uniaxially pressed at 360 MPa and sintered in air at different selected temperatures (1150–1250 °C) for 5 h with a fixed heating rate of 100 °C h^{-1}.

The anode-supported BCZYZn bi-layer (φ15 mm) was prepared by a dry-pressing method. NiO + BCZYZn mixture (60:40 in weight %) was pre-pressed at 200 MPa as a substrate. Then loose BCZYZn powder, calcined at 1000 °C for 5 h to form a pure perovskite oxide, was uniformly distributed onto an anode substrate, co-pressed at 250 MPa and sintered subsequently at 1250 °C for 5 h to densitify the BCZYZn membrane. $Ba_{0.5}Sr_{0.5}Zn_{0.2}Fe_{0.8}O_{3-\delta}$ perovskite cathode powder was also synthesized by the modified Pechini method [23] using $Ba(NO_3)_2{\cdot}9H_2O$, $Sr(NO_3)_2$, ZnO (99.95%, Shanghai), and $Fe(NO_3)_3{\cdot}9H_2O$ as precursors, followed by calcinations at 950 °C for 5 h. The BSZF slurry was applied to the electrolyte by printing and then fired at 1000 °C for 3 h to form a porous cathode.

The phase identification of calcined BCZYZn powders, sintered anode-electrolyte bi-layer and prepared BSZF powders was carried out by a Philips X'Pert Pro Super Diffractometer system using Cu Kα radiation (λ = 1.5418 Å). The relative densities were measured by Archimedes method. Theoretical densities were calculated using experimental lattice parameters and chemical formula $BaCe_{0.5}Zr_{0.3}Y_{0.16}Zn_{0.04}O_{3-\delta}$ (δ = 0.12). Microstructures were examined by a KYKY 1010B scanning electron microscope. The samples were analyzed by scanning electron microscope (SEM, JEOL JSM-6400) equipped with EDX for compositional analysis. Single cells were tested from 550 to 700 °C in a home-developed-cell-testing system with humidified hydrogen (~3% H_2O) as fuel and the static air as oxidant, respectively. The flow rate of fuel gas was about 40 ml min^{-1}. The cell voltages and output current of the cells were measured with digital multi-meters (GDM-8145). AC impedance spectroscopy (Chi604c, Shanghai Chenhua) was performed on the cell under open-current conditions from 550 to 700 °C. A scanning electron microscope (SEM) was used to observe the microstructure of the cells after testing.

3. Results and discussion

3.1. Powder characterizations

Fig. 1 shows the XRD pattern for the BCZYZn powders calcined at 850, 900, 1000, and 1100 °C for 5 h. With the calcining temperature

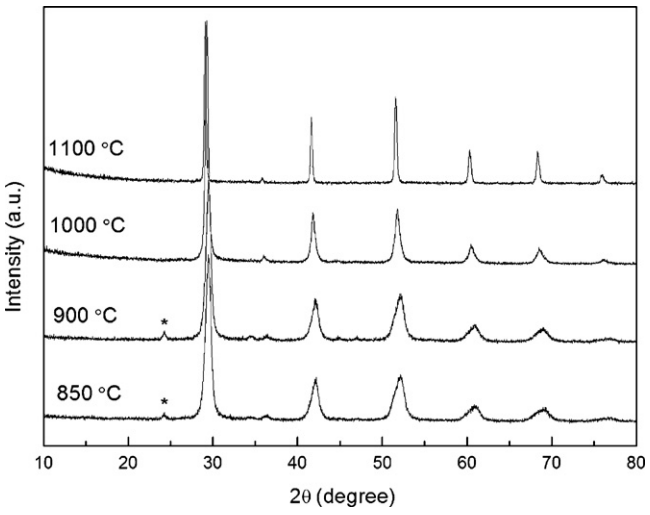

Fig. 1. XRD patterns for perovskite $BaCe_{0.5}Zr_{0.3}Y_{0.16}Zn_{0.04}O_{3-\delta}$ (BCZYZn) powders calcined at different temperatures (850–1100 °C) for 5 h. *$BaCO_3$.

increasing, the XRD peaks grow sharper, revealing an enhancement in crystallization of the amorphous phase and the primary crystallite size. A slight amount of second phase $BaCO_3$ was detected as the powders calcined at 850 and 900 °C for 5 h. However, the second phase $BaCO_3$ dissolved and a pure perovskite phase was formed when the samples were sintered at or above 1000 °C for 5 h. The XRD results of BCZYZn indicated that the calcining temperature of BCZYZn powder should be at or above 1000 °C to obtain the pure perovskite oxide. Fig. 2 shows the SEM image of the as-prepared BCZYZn powder. These agglomerates consisted of porous particles of the as-prepared material. This porous structure was typical for powders prepared by the combustion technique. The walls were very thin and the porous structure could be easily crushed to fine powder.

3.2. Chemical stability

In order to investigate the chemical stability of materials against CO_2, powder samples of BCZYZn calcined at 1000 °C for 5 h were

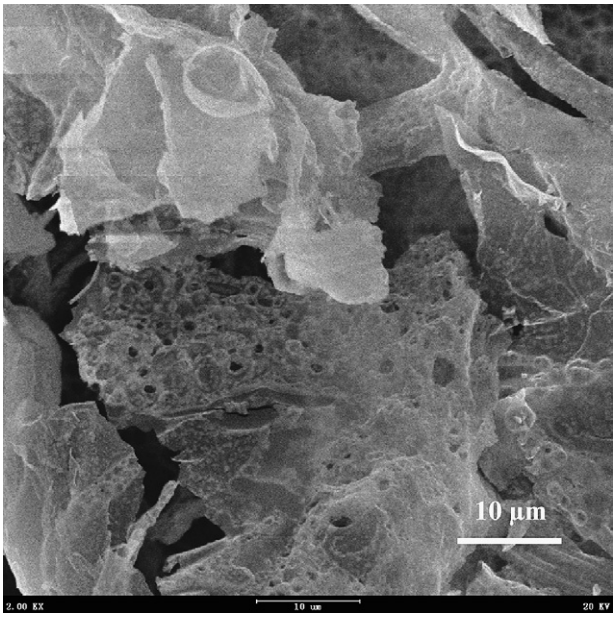

Fig. 2. SEM image of the as-prepared BCZYZn powder.

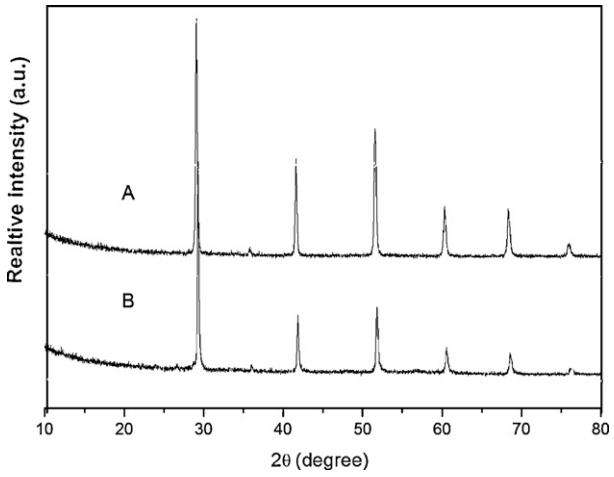

Fig. 3. XRD patterns of BCZYZn powders calcined at 1000 °C before (A) and after (B) exposing to CO_2 atmosphere at 1200 °C.

held in the tube furnace at 1200 °C and exposed to flowing carbon dioxide for 1 h. Fig. 3 shows the XRD patterns of powders before (A) and after (B) exposing to CO_2 atmosphere at 1200 °C. The XRD patterns before (A) and after (B) treated in CO_2 atmosphere were almost identical to each other, showing relative stability against carbon dioxide. The behavior here was consistent with that reported by Tao and Irvine [13]. The Zn action in enhancing CO_2 tolerance of $BaCeO_3$ was interpreted by Tao and Irvine [13] according to the investigation of gravimetric behavior in CO_2 atmosphere on cycling up to 1200 °C. In general, rare earth-doped $BaCeO_3$ has been found to be unstable in CO_2 and/or H_2O containing atmospheres under fuel cell operating conditions. Some investigators introduced Zr to substitute Ce for increasing resistance against carbon dioxide and steam. Zuo et al. [20] investigated the chemical stability of $BaZr_{0.1}Ce_{0.7}Y_{0.2}O_{3-\delta}$ in a CO_2-containing atmosphere. A slight amount of second phase $BaCO_3$ was detected as the powder samples exposed to 2% CO_2 (balanced with H_2) at 500 °C for 1 week. It may be ascribed to the small amount of Zr substitution. However, accompanied by the increase of Zr magnitude, the sintering temperature increased to above 1500 °C that resulted in poor quality and higher cost.

3.3. Sintering behavior

As shown in Fig. 4, the SEM photographs of the fracture surfaces of BCZYZn samples sintered at different temperatures for 5 h clearly show the effects of sintering temperature on densification, microstructure and grain growth. From the images, it can be seen that the grain size increased and the porosity decreased with increasing sintering temperature. The grain size varied from about 1–2 μm at the lower sintering temperature (1150 °C) to 6–10 μm at 1250 °C. This feature of the microstructure indicated the materials were densely sintered. When the sintering temperature increased from 1150 to 1200 °C, the relative density of the samples increased from 95.3 to 97.4%. As the sintering temperature further increased to 1250 °C, the relative density (97.7%) had hardly any change, indicating that the sample was almost fully sintered dense at 1200 °C for 5 h. It is worthy to note that even sintered at the temperature of 1150 °C, the relative density still could reach 95.3%. This sintering temperature of BCZYZn is about 200 °C lower than that without Zn dopant.

The sintering temperature for achieving dense BCZYZn membrane in our experiment was proved to be 1200 °C, lower than 1325 °C employed by Tao and Irvine through solid-state reaction process [13]. It was obvious that zinc certainly played an important role in both increasing chemical stability and decreasing sintering temperature. The Zn action in decreasing sintering temperature was interpreted by Haile and coworker [12] and Tao and Irvine [13] according to the investigation of sintering shrinkage behavior of the pellets as a function of firing temperature. In addition, the further lowered sintering temperature represented in this work illustrated the advantages of the soft chemical route for powder preparation, compared to the conventional solid-state reaction.

From the viewpoint of proper configuration design, high-performance fuel cells require thin dense electrolyte membrane and porous electrode. The overview of the microstructure of the anode supported electrolyte membrane with a BSZF cathode is shown. The thickness of the BCZYZn layer was about 30 μm, and that of BSZF cathode layer was about 10 μm. Both the anode and the cathode exhibited uniform microstructure and good adherence to the electrolyte. The achievement of dense electrolyte layer needed only 1200 °C for the BCZYZn powders prepared by soft chemical routes. This sintering temperature was remarkably lower than that for obtaining dense SDC (1300 °C [25]) and YSZ membrane (1400 °C [26]).

3.4. Elemental distribution

Fig. 5 shows the Zn (b), Ba (c), Ce (d), Zr (e), and Y (f) X-ray peak intensities versus position in the perovskite BCZYZn material sintered at 1250 °C for 5 h. These EDX images suggested that elemental distribution was homogeneous without any separate regions rich, which was consistent with the XRD results. The homogeneous distribution of Zn in the BCZYZn sample indicated that zinc did enter the bulk rather than stayed at the grain boundary. The ionic size of

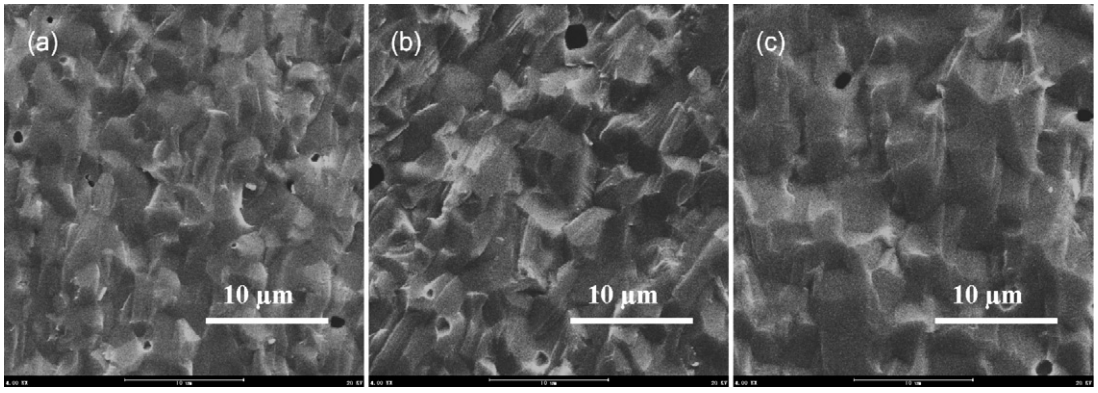

Fig. 4. SEM images of the fracture surface of BCZYZn samples sintered at different temperature for 5 h (a–c: 1150, 1200, and 1250 °C, respectively).

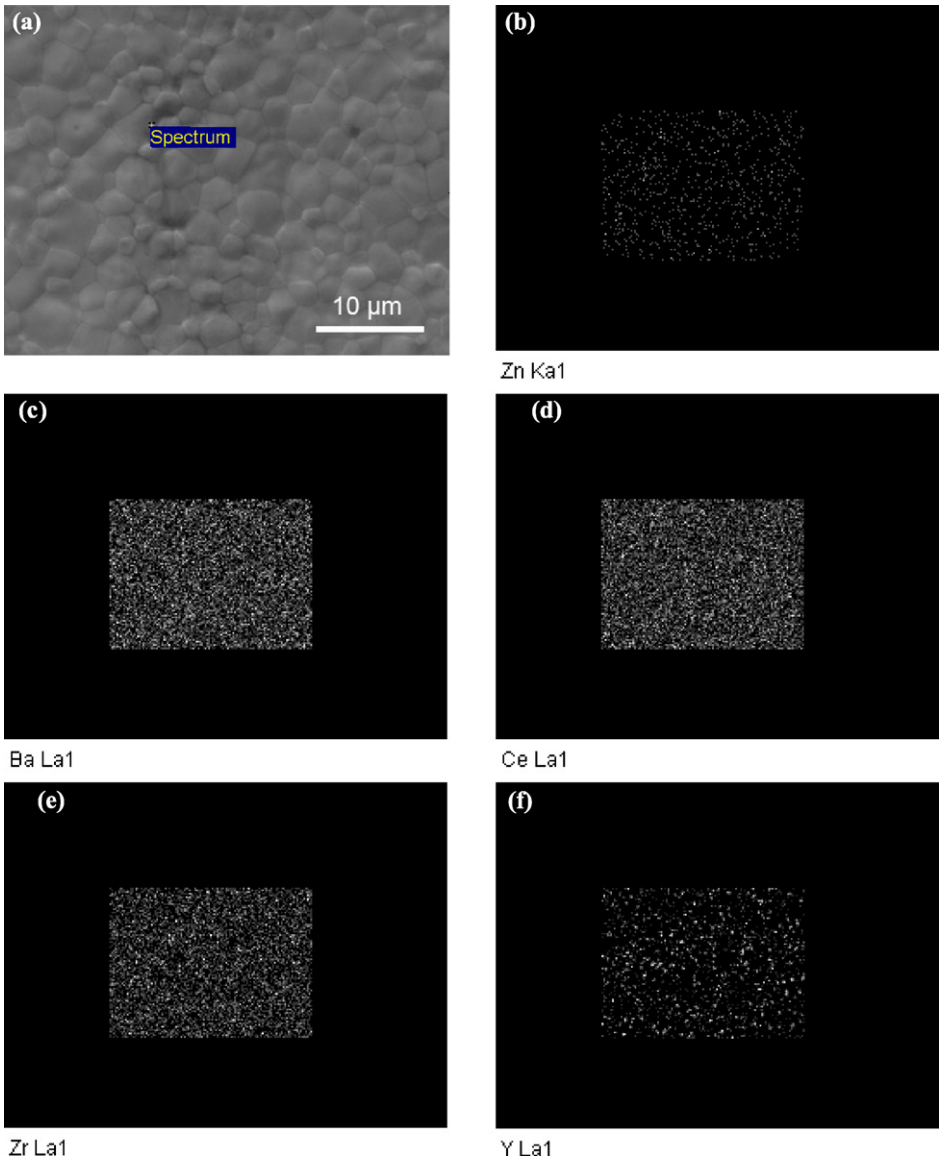

Fig. 5. SEM mapping of the BCZYZn sample calcined at 1250 °C for 5 h in air.

Zr^{4+} and Zn^{2+} ions is 0.72 and 0.74 Å, respectively, which are fairly close. Tao and Irvine [27] confirmed that Zn entered the lattice on firing forming a solid solution with the Zn expected to occupy the B-site. An exposed surface SEM image of the BCZYZn sample sintered at 1250 °C for 5 h is given in Fig. 5(a). The sintered ceramic was completely dense and the grains were quite uniform in the size of 6–10 μm. The grain boundaries of the samples were clear, along which the grains grew perfectly straight.

3.5. Cell performance

As shown in Fig. 6, the as-synthesized powder of BSZF exhibits a cubic perovskite phase structure [23]. Fig. 6 also presents the XRD patterns of anode/electrolyte bi-layer sintered at 1250 °C for 5 h. It could be clearly seen that there were only peaks corresponding to BCZYZn in electrolyte membrane and to NiO and BCZYZn in the anode substrate, but no evidence for the formation of other substance.

Fig. 7(a) shows the SEM image of surface morphology of the as-prepared tri-layer cell of BCZYZn electrolyte on the porous anode

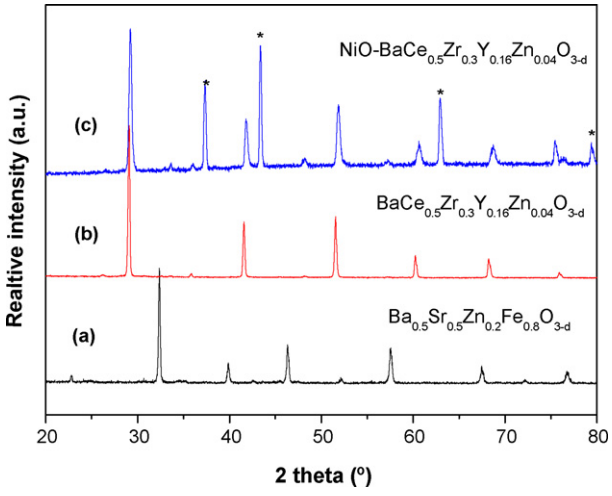

Fig. 6. XRD patterns for (a) the perovskite $Ba_{0.5}Sr_{0.5}Zn_{0.2}Fe_{0.8}O_{3-\delta}$ (BSZF) powders, the bi-layer of (b) BCZYZn membrane and (c) NiO–BCZYZn anode substrate. *NiO.

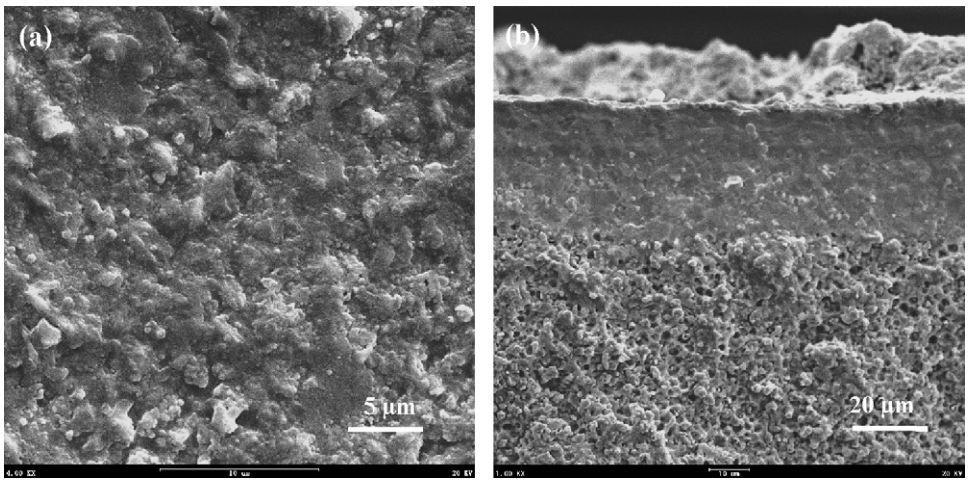

Fig. 7. SEM micrographs of cell after testing: (a) the surface of electrolyte and (b) the cross-section of cell with a 30-μm thick BCZYZn membrane.

support after testing. It can be seen that the BCZYZn membrane was completely dense. There was no obvious pores and cracks on the surface. From the cross-section view of the co-fired BCZYZn membrane (Fig. 7(b)), it was found that the BCZYZn membrane was about 30–40 μm thick.

Fig. 8 presents the *I–V* and *I–P* characteristics of the as-prepared cell, the SEM image of which is shown in Fig. 7. The almost linear *I–V* curve implied little electrode polarization. And also, we could deduce that the voltage drop of the cell was mostly from IR fall across the BCZYZn electrolyte because both anode and cathode materials exhibited much higher conductivity than electrolyte materials [19]. The open-circuit voltages (OCV) of 1.00 V at 700 °C, 1.03 V at 650 °C, 1.06 V at 600 °C and 1.08 V at 550 °C indicated that the electrolyte membrane was sufficiently dense. Peak power densities were 236, 185, 122, and 79 mW cm^{-2} at 700, 650, 600, and 550 °C, respectively. From the slopes the total resistances were calculated by linear fitting to be 1.10, 1.46, 2.05 and 3.35 Ω cm^2 at 700, 650, 600, and 550 °C, respectively. Assuming the cell resistance mostly came from the electrolyte the conductivity of BCZYZn (30 μm) were 2.73×10^{-3}, 2.05×10^{-3}, 1.46×10^{-3}, and 0.89×10^{-3} S cm^{-1} at 700, 650, 600, and 550 °C, respectively. The values were about 10 times smaller than that mentioned above [13] (over 10 mS cm^{-1} above 600 °C), which seemed incredible.

Fig. 7(b) shows the cross-section view of the cell, Ni–BCZYZn/BCZYZn/BSZF after testing. As can be seen, the BCZYZn electrolyte was about 30–40 μm in thickness, quite dense and adhered very well to the layers of anode and cathode. It surely should be expected to get a higher power density than the values mentioned above, as here we have pretty thin electrolyte and cathode layers. The reason may mainly come from the anode layer. As we can see from Fig. 7(b), the anode layer was rather dense instead of porous, indicating incomplete reduction of the NiO into metal Ni. The dense layer of BCZYZn + NiO would have rather large thickness and much poorer conductivity compared with BCZYZn electrolyte layer. Therefore the cell exhibited very high resistance and thus rather low output power density.

In order to evaluate the performance of perovskite BSZF working as a cathode in a PCMFC, the impedance spectra of the as-prepared cells under open-current conditions at different temperatures is shown in Fig. 9(a). In these spectra, the intercepts with the real axis at low frequencies represent the total resistance of the cell and the value of the intercept at high frequency is the electrolyte resistance, while the difference of the two values corresponds to the sum of the resistance of the two interfaces: the cathode-electrolyte interface and the anode–electrolyte interface. As expected, the increase of the measurement temperature resulted in a significant reduction of the interfacial resistances, typically from 1.89 Ω cm^2 at 550 °C to

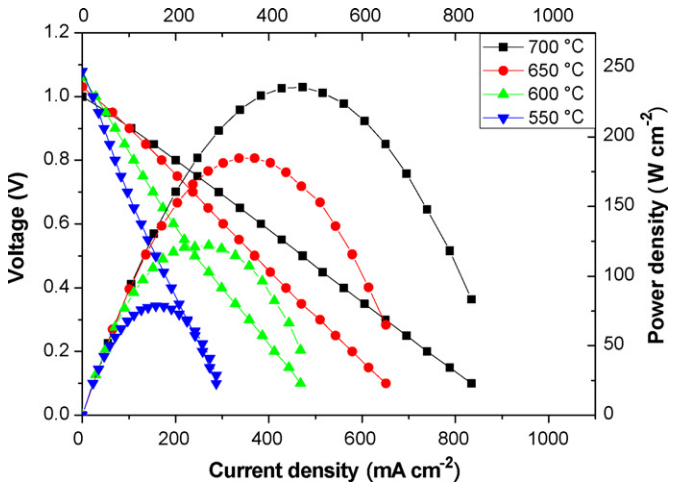

Fig. 8. Performance of the as-prepared cell with hydrogen at different temperatures.

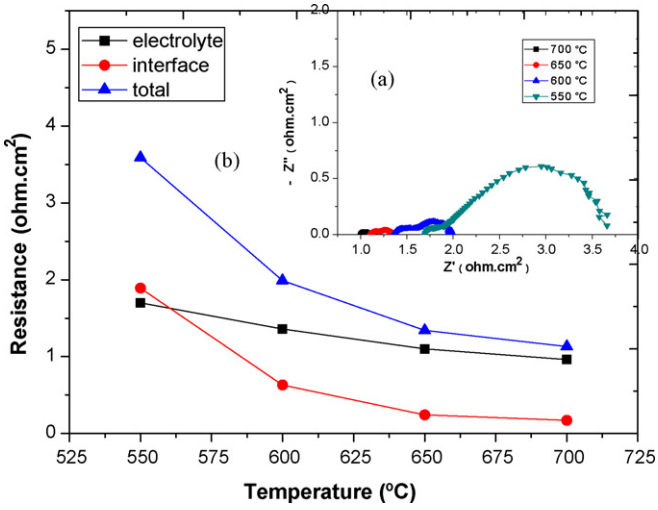

Fig. 9. (a) Impedance spectra and (b) the interfacial polarization resistances, electrolyte resistances, and total resistances determined from the impedance spectra of the as-prepared cell measured under open-circuit conditions at different temperatures.

0.17 Ω cm^2 at 700 °C. The results indicated that the perovskite BSZF cathode was a good candidate for operation at or below 700 °C. Further, Fig. 9(b) shows that the cell performance was influenced by the interfacial resistances, especially at temperatures below 550 °C, where the cell performance was essentially determined by the interfacial resistances. At 550 °C, the polarization resistance of the electrodes was 1.89 Ω cm^2 whereas the resistance of the electrolyte was only 1.7 Ω cm^2. So we can deduce that development of proper cathode materials is a grand challenge for developing the low-temperature PCMFCs.

4. Conclusions

A stable, easily sintered perovskite oxide $BaCe_{0.5}Zr_{0.3}Y_{0.16}Zn_{0.04}O_{3-\delta}$ (BCZYZn) as an electrolyte for protonic ceramic membrane fuel cells with $Ba_{0.5}Sr_{0.5}Zn_{0.2}Fe_{0.8}O_{3-\delta}$ perovskite cathode was investigated. The BCZYZn perovskite electrolyte synthesized by a modified Pechini method exhibited higher sinterability and reached 97.4% relative density at 1200 °C for 5 h in air, which is about 200 °C lower than that without Zn dopant. A laboratory-sized tri-layer cell of NiO–BCZYZn/BCZYZn (30 μm)/BSZF, not yet optimized for performance, was operated from 550 to 700 °C fed with humidified H_2 (~3% H_2O). An open-circuit potential of 1.00 V and a maximum power density of 236 mW cm^{-2} were achieved at 700 °C. The polarization resistance of the electrodes was as low as 0.17 Ω cm^2 at 700 °C. These results indicate that the perovskite BSZF cathode is a good candidate for operation at or below 700 °C, and that proton conducting electrolyte BCZYZn with BSZF cathode is a promising material system for the next generation solid oxide fuel cells. The results will be expected to open up a new phase of the research on the proton conducting electrolyte-based solid oxide fuel cells (SOFCs).

Acknowledgements

The authors gratefully acknowledge the support of this research by National Natural Science Foundation of China under contract No. 50572099, Chinese Research Foundation for the Doctors (20040358025).

References

[1] G. Meng, G. Ma, Q. Ma, R. Peng, X. Liu, Solid State Ionics 178 (2007) 697.
[2] A.F. Sammells, R.L. Cook, J.H. White, J.J. Osborne, R.C. MacDuff, Solid State Ionics 52 (1992) 111.
[3] A.K. Demin, P.E. Tsiakaras, V.A. Sobyanin, S.Yu. Hramova, Solid State Ionics 152–153 (2002) 555.
[4] H. Iwahara, H. Uchida, K. Ono, K. Ogaki, J. Electrochem. Soc. 135 (1988) 529.
[5] J. Wang, W. Su, D. Xu, T. He, J. Alloys Compd. 421 (2006) 45.
[6] J. Wu, S.M. Webb, S. Brennan, S.M. Haile, J. Appl. Phys. 97 (2005), 054101(1).
[7] H. Iwahara, T. Yajima, T. Hibino, H. Ushida, J. Electrochem. Soc. 140 (1993) 1687.
[8] N. Bonanos, Solid State Ionics 53–56 (1992) 967.
[9] S. Wienströer, H.D. Wiemhöfer, Solid State Ionics 101–103 (1997) 1113.
[10] K.D. Kreuer, Solid State Ionics 125 (1999) 285.
[11] H.G. Bohn, T. Schober, J. Am. Ceram. Soc. 83 (2000) 768.
[12] P. Babilo, S.M. Haile, J. Am. Ceram. Soc. 88 (2005) 2362.
[13] S.W. Tao, J.T.S. Irvine, Adv. Mater. 18 (2006) 1581.
[14] R. Peng, Y. Wu, L. Yang, Z. Mao, Solid State Ionics 177 (2006) 389.
[15] T. Hibino, A. Hashimoto, M. Suzuki, M. Sano, J. Electrochem. Soc. 149 (2002) A1503.
[16] Q. Ma, R. Peng, Y. Lin, J. Gao, G. Meng, J. Power Sources 161 (2006) 95.
[17] M. Koyama, C.J. Wen, K. Yamadab, J. Electrochem. Soc. 147 (1) (2000) 87.
[18] T. Wu, R. Peng, C. Xia, Solid State Ionics (2007), doi:10.1016/j.ssi.2007.12.005.
[19] B. Lin, S. Zhang, L. Zhang, L. Bi, H. Ding, X. Liu, J. Gao, G. Meng, J. Power Sources 177 (2008) 330.
[20] C. Zuo, S. Zha, M. Liu, M. Hatano, M. Uchiyama, Adv. Mater. 18 (2006) 3318.
[21] H. Yamaura, T. Ikuta, H. Yahiro, G. Okada, Solid State Ionics 176 (2005) 269.
[22] H. Wang, C. Tablet, A. Feldhoff, J. Caro, Adv. Mater. 17 (2005) 1785.
[23] B. Wei, Z. Lu, X. Huang, Z. Liu, J. Miao, N. Li, W. Su, J. Am. Ceram. Soc. 90 (2007) 3364.
[24] B. Wei, Z. Lu, X. Huang, M. Liu, N. Li, W. Su, J. Power Sources 176 (2008) 1.
[25] Q.L. Liu, K.A. Khor, S.H. Chan, J. Power Sources 161 (2006) 123.
[26] S. de Souza, S.J. Visco, L.C. De Jonghe, J. Electrochem. Soc. 144 (1997) L35–L37.
[27] S. Tao, J.T.S. Irvine, J. Solid State Chem. 180 (2007) 3493.